

Original Article

## miR-378a-5p represses Barrett's esophagus cells proliferation, migration and invasion through targeting TSPAN8

Xudong Xie, Duo Wei\*

Department of Gastroenterology Ward 2, Xianyang Hospital of Yan'an University, Xianyang, Shaanxi 712000, China

### Article Info

### Abstract



#### Article history:

Received: September 17, 2023

Accepted: December 06, 2023

Published: February 29, 2024

Use your device to scan and read the article online



Barrett's esophagus (BE) belongs to a pathological phenomenon occurring in the esophagus, this paper intended to unveil the underlying function of miR-378a-5p and its target TSPAN8 in BE progression. GEO analysis was conducted to determine differentially expressed genes in BE samples. Non-dysplastic metaplasia BE samples, high-grade dysplastic BE samples and controls were collected from subjects. CP-A and CP-B cells were exposed to bile acids (BA) to mimic gastroesophageal reflux in BE cells. RT-qPCR as well as western blot were applied for verifying expressions of miR-378a-5p, TSPAN8, CDX2 and SOX9. CCK-8, wound scratch together with Transwell assays were exploited for ascertaining cell proliferation, migration as well as invasion. The targeted relationship of miR-378a-5p and TSPAN8 could be verified by correlation analysis, dual-luciferase reporter experiment, and rescue experiments. Through analyzing GSE26886 dataset, we screened the most abundantly expressed gene TSPAN8 in BE samples. miR-378a-5p was reduced whereas TSPAN8 was elevated in CP-A as well as CP-B cells after triggering with BA. Knocking down TSPAN8 could counteract BA-triggered enhancement in BE cell proliferation, migration along with invasion. miR-378a-5p could suppress BE cell proliferation, and migration along with invasion via targeting TSPAN8. In BE, miR-378a-5p targeted TSPAN8 to inhibit BE cell proliferation, and migration along invasion. miR-378a-5p deletion or elevation of TSPAN8 may be key point in regulating CDX2 and SOX9 levels, thereby promoting BE formation.

**Keywords:** Barrett's esophagus, Dysplastic cells, Metaplastic cells, miR-378a-5p, TSPAN8

## 1. Introduction

Barrett's esophagus (BE) belongs to a pathological appearance in which the squamous epithelium of the reduced esophagus can be replaced by a simple columnar epithelium, with or without intestinal epithelial metaplasia [1]. Among them, patients with intestinal epithelial metaplasia are precancerous lesions of esophageal adenocarcinoma [2]. In developed countries, about 9% of white men over 50 years of age have BE; 0.5% to 1% of these patients will develop esophageal adenocarcinoma [3]. With the increasing aging of society and the increasing awareness of BE, research on BE has received increasing attention for the past few years. It has been documented that 2.44% of patients undergoing endoscopy in China are diagnosed with BE, and that the occurrence of BE is associated with gastroesophageal reflux disease, in which gastric and/or duodenal contents reflux into the esophagus, triggering mucosal inflammation and eventual development of BE [4, 5]. Nevertheless, the exact molecular mechanism underlying BE progression is unclear.

Recently, with the development and widespread application of techniques to detect the microenvironment in the esophagus, such as 24 h pH testing and bilirubin monitoring in the esophagus, the role of bile reflux in the formation of BE has gradually attracted attention [6]. It has been shown that acid exposure can increase the risk of

esophageal mucosal carcinogenesis by affecting a series of processes such as cell division and decay [7, 8]. However, the specific cellular and molecular mechanisms by which reflux-associated injury leads to the development of BE are still not well understood. Therefore, research on BE and associated esophageal adenocarcinoma should be emphasized.

Bile acids (BA) contain lithocholic acid, deoxycholic acid (DCA), cholic acid, and goose deoxycholic acid [9]. Of these, the main component that exerted cellular damage was DCA, and DCA was the main component of BA [10]. In numerous cellular experiments, it has also been confirmed that DCA has a crucial role in promoting the BE progression [11, 12]. Previous studies used BA to induce immortalized BE cells, such as CP-A and CP-B, for the construction of BE in vitro models [13, 14]. In the present study, we designed to expose CP-A and CP-B cells to BA to stimulate gastroesophageal reflux which was applied to mimic BE environment in vitro. Then, the CCK-8, wound scratch, Transwell Chamber along western blot assays were exploited to certify BE cell development.

## 2. Materials and methods

### 2.1. GEO analysis

All microarray data in MINiML format was downloaded from the GEO database (<https://www.ncbi.nlm.nih.gov>).

\* Corresponding author.

E-mail address: [weiduoyadxyyy@163.com](mailto:weiduoyadxyyy@163.com) (D. Wei).Doi: <http://dx.doi.org/10.14715/cmb/2024.70.2.14>

gov/geo/). mRNA differential expression could be studied with the help of the limma package of R software (version: 3.40.2). Adjusted P values could be analyzed in GEO to redress for false positive results. “Adjusted  $P < 0.05$  and  $\log_2$  (fold change)  $> 1$  or  $\log_2$  (fold change)  $< -1$ ” was considered to be the threshold mRNA differential expression screen. Functional enrichment analysis could be performed on the data to further verify the potential role of potential targets. Gene ontology (GO) is an extensively applied tool for functional gene annotation, especially molecular functions (MF), biological pathways (BP) as well as cellular components (CC). Kyoto Encyclopedia of Genes and Genomes (KEGG) enrichment analysis can be adopted to analyze gene functions along with associated high-level genomic functional information. In order to better comprehend the oncogenic potential of target genes, the ClusterProfiler package in R was adopted for analyzing the GO function of possible mRNAs as well as the enriched KEGG pathway. Principal component analysis (PCA) maps could be mapped by the R package; expression heat maps could be exhibited by the R package pheatmap.

## 2.2. Sample collection

24 cases diagnosed with BE from January 2016 to December 2020 at our hospital were included, 13 of which were non-dysplastic BE and 11 were dysplastic BE. 15 healthy esophageal squamous epithelial tissue specimens from the same period were included as control group. No preoperative treatment was performed in all cases. All patients signed an informed consent form. The study was approved by the ethics committee.

## 2.3. Cell culture, cell transfection and bile acids treatment

BE cell lines (CP-A and CP-B) were acquired from ATCC (USA) and inoculated with 1640 medium which contained 10% fetal bovine serum and maintained at 37°C with 5% CO<sub>2</sub>. CP-A together with CP-B cells at logarithmic growth stage were added with acid exposure along with BA (100 μM) to construct BE in vitro model.

Lipofectamine 2000 reagent was mixed with si-NC, si-TSPAN8, ov-NC, ov-TSPAN8, mimics-NC, mimics, inhibitor-NC and inhibitor (GenePharma, Shanghai, China) for 24 h of cultivation at 37°C. TSPAN8 or miR-378a-5p expression could be detected by RT-qPCR for verifying the transfection efficiency.

## 2.4. RT-qPCR analysis

After cell lysis using TRIzol reagent, total RNA was extracted and then assayed for RNA concentration. Then, the PCR amplification process was implemented by thermal cycling. Among them, miR-378a-5p and TSPAN8 were amplified with U6 and GAPDH worked as the internal reference for each amplification. The amplification results were analyzed using ABI 7500 and the relative expression could be calculated with the help of the  $2^{-\Delta\Delta CT}$  method.

## 2.5. Western blot analysis

Cells were gathered and lysed in RIPA buffer. Protein concentration could be determined with the help of BCA kit. The protein content (50 μg) was separated by 10% SDS-PAGE electrophoresis and then shifted to PVDF membranes. 5% skimmed milk was adopted for blocking at room temperature for 2 h for blocking the non-speci-

fic binding of antibodies. Diluted primary antibodies were then added and cultivated overnight at 4°C. On the next day, the membranes were rewarmed at room temperature, and IgG-HRP secondary antibody was added and incubated for 2 h. ECL luminescent solution was supplemented and optical density values were quantified by Image-J software. The ratio of GAPDH protein expression was used as an internal reference.

## 2.6. CCK-8 analysis

The 96-well plates were inoculated with  $3 \times 10^3$  cells/well CP-A or CP-B cells after the experimental treatment. Afterward, 10 μL of CCK-8 solution could be treated in each well for 2 h of incubation avoiding lights. The absorbance could be measured at 450 nm with the help of an enzyme marker.

## 2.7. Wound scratch assay

Cells were planted into 6-well plates and scratched on the cell plates using a sterile pipette. The scratch was placed under the microscope and the width of the scratch was photographed. After incubation for 48 h, the cultured cell plates were inverted under the microscope to take pictures of the scratch healing degree and recorded, which was used to calculate the scratch distance of each group.

## 2.8. Transwell assay

The above chamber of the Transwell could be pre-layered with Matrigel matrix and dried naturally. Then, 100 μl of cell suspension ( $5 \times 10^4$  cells/ml) was placed on the upper chamber of Transwell and 500 μl of complete medium was put on the lower chamber. After cultivation for 24 h at room temperature, the cells were placed in paraformaldehyde solution and fixed for 30 min. Next, cells received staining by crystal violet for 20 min. After washing, the cells could be counted.

## 2.9. Dual-luciferase reporter assay

The wild type (WT), as well as mutant type (MUT) of TSPAN8, were designed by Shanghai GenePharma and cloned into pMIR-report plasmids named WT-TSPAN8 and MUT-TSPAN8, respectively. CP-A and CP-B cells were inoculated in 24-well plates ( $2.5 \times 10^4$  cells/well), followed by co-transfection with WT-TSPAN8 or MUT-TSPAN8 together with mimics-NC or mimics using Lipofectamine 2000 reagent. Then, firefly luciferase reaction working solution was added and the fluorescence intensity of firefly was detected by GENios Pro multifunctional enzyme marker.

## 2.10. Statistical analysis

The data were analyzed with the help of SPSS 22.0. The measurement data were exhibited as mean  $\pm$  standard deviation (SD). Two-by-two analysis was implemented using an independent samples t-test, and ANOVA test was adopted for data analysis between multiple groups. Differences were significant when  $P < 0.05$ .

## 3. Results

### 3.1. Differentially expressed genes in BE samples

The GSE26886 dataset contained 69 frozen esophageal squamous epithelium specimens (20 cases of BE patients, 21 cases of esophageal adenocarcinoma patients, 19 healthy subjects as well as 9 cases of esophageal squamous

cell carcinoma). After analyzing the dataset, the boxplot of the normalized data is shown in Figure 1A. Meanwhile, the PCA outcomes before and after batch removal were depicted in Figures 1B and 1C. Furthermore, the volcano plot was demonstrated in Figure 1D (red dots indicated up-regulated genes while blue dots indicated down-regulated genes). The volcano results revealed the most up-regulated TSPAN8 gene in BE samples. Then, the heatmap plot in Figure 1E indicated differentially expressed genes (the top 50 up-regulated as well as top 50 down-regulated genes). Finally, the KEGG and GO analysis in Figure 1F showed that focal adhesion, extracellular matrix organization and extracellular structure organization were enriched in up-regulated genes; whereas, salmonella infection, endocytosis, axon guidance and epidermis development were enriched in down-regulated genes.

### 3.2. miR-378a-5p and TSPAN8 served as feasible biomarkers for BE diagnosis

After collecting esophageal squamous epithelium specimens from 15 healthy subjects and 24 BE cases (13 non-dysplastic BE subjects and 11 high-grade dysplastic BE subjects), the abnormal expressions of miR-378a-5p and TSPAN8 were detected. As displayed in Figure 2A, miR-378a-5p presented decreased in BE specimens compared with healthy samples; meanwhile, miR-378a-5p was further declined in high-grade dysplastic BE samples in comparison with non-dysplastic metaplasia specimens. The ROC result in Figure 2B elucidated that miR-378a-5p could discriminate BE cases from healthy controls with an area under the curve of 0.9778 (95% CI = 0.9413~1.000,  $P < 0.001$ ). Inversely, TSPAN8 was dramatically increased in BE cases in relation to healthy subjects, which was further enhanced in high-grade dysplastic BE specimens as compared with non-dysplasia BE cases (Figure 2C). To verify the diagnostic value of TSPAN8 in BE, we performed ROC analysis. As depicted in Figure 2D, TSPAN8 could distinguish BE specimens from healthy cases with an AUC of 0.8528 (95% CI = 0.7350~0.9705,  $P < 0.001$ ). Finally, the association between miR-378a-5p and TSPAN8 in BE samples was analyzed with the help of Spearman's correlation analysis. The inverse correlation was discovered in miR-378a-5p and TSPAN8 ( $r = -0.6649$ ,  $P < 0.001$ , Figure 2E). In a word, miR-378a-5p together with TSPAN8 might serve as feasible indicators for BE detection and participate in BE progression.

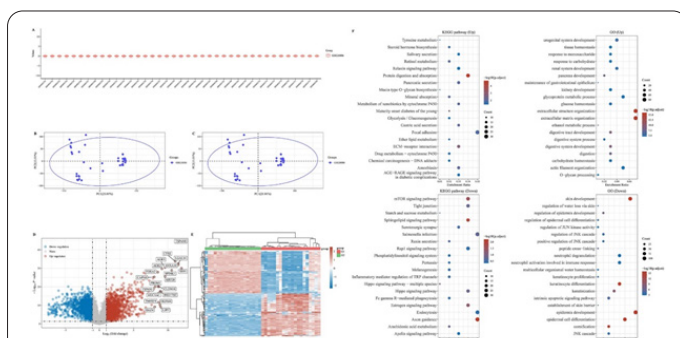


**Fig. 1.** GEO analysis verified differentially expressed genes in BE samples. (A) The boxplot of the normalized data. (B) Principal component analysis (PCA) outcomes previous to batch removal of multiple datasets. (C) PCA outcomes followed by batch removal. (D) Volcano plot indicated dysregulated genes. (E) The heatmap of the differential gene expressions. (F) Functional enrichment.

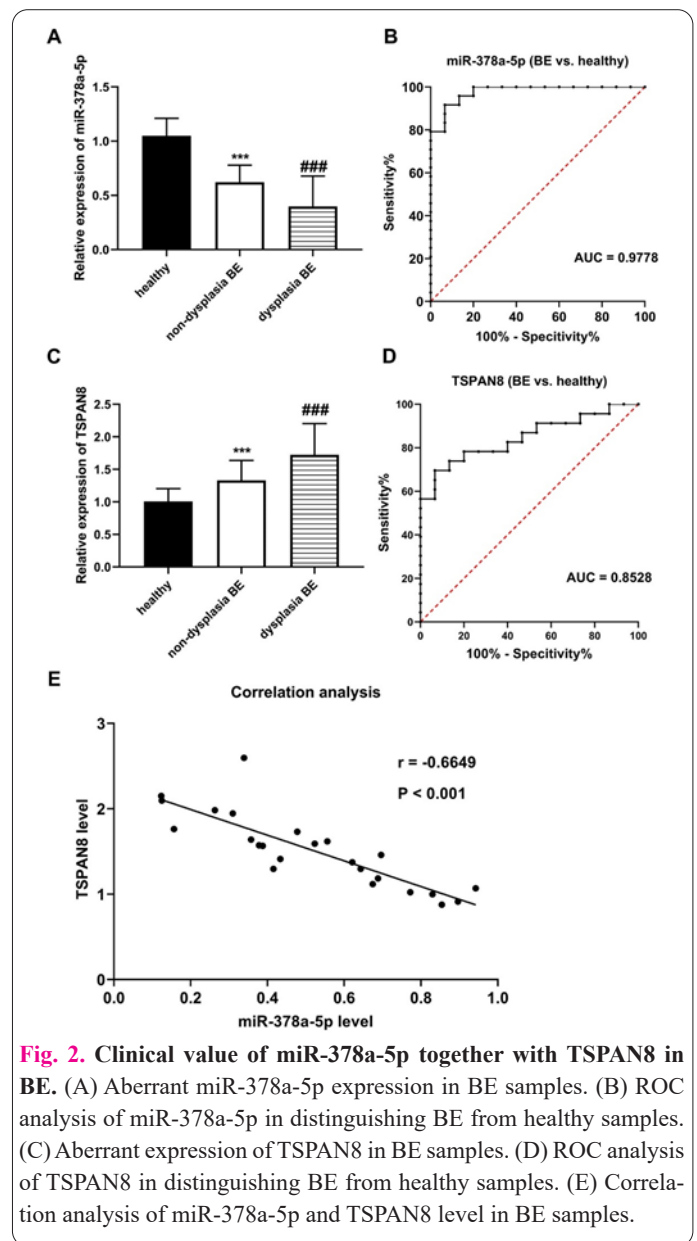


**Fig. 2.** Clinical value of miR-378a-5p together with TSPAN8 in BE. (A) Aberrant miR-378a-5p expression in BE samples. (B) ROC analysis of miR-378a-5p in distinguishing BE from healthy samples. (C) Aberrant expression of TSPAN8 in BE samples. (D) ROC analysis of TSPAN8 in distinguishing BE from healthy samples. (E) Correlation analysis of miR-378a-5p and TSPAN8 level in BE samples.

### 3.3. Knockdown of TSPAN8 depleted BE development

CP-A and CP-B cells were treated with BA to mimic BE in vitro model. After triggering with BA, TSPAN8, CDX2 and SOX9 levels were overtly enhanced in CP-A and CP-B cells, implying the construction of BE model was successful (Figure 3A). Then, we knocked down TSPAN8 by transfection with si-TSPAN8 plasmid. As demonstrated in Figure 3B, in comparison with si-NC group, si-TSPAN8 transfection could markedly hindered TSPAN8, CDX2 and SOX9 expression. Moreover, the CCK-8 assay in Figure 3C suggested that BA treatment promoted BE cell proliferation in a time-dependent manner; however, silencing of TSPAN8 could counteract the enhancement in BE cell proliferation induced by BA treatment. Similarly, the wound scratch and Transwell experiments in Figures 3D and 3E revealed that BA stimulation promoted CP-A and CP-B cell migration and invasion; whereas, the acceleration could be partially reversed after co-transfection with si-TSPAN8 plasmid. Collectively, the above-mentioned experiments implied that TSPAN8 knockdown might deplete BE development.

### 3.4. TSPAN8 was targeted by miR-378a-5p

Through TargetScan online tool (<https://www.tar->

getscan.org/), we observed the underlying binding sequences between miR-378a-5p and TSPAN8 (Figure 4A). Then, the dual-luciferase reporter assay could be exploited for further verifying the targeted association between miR-378a-5p and TSPAN8. In WT-TSPAN8-transfection groups, co-transfection with miR-378a-5p mimics could markedly reduce the luciferase intensity relative to mimics-NC group. However, no significant differences were discovered in MUT-TSPAN8-transfection

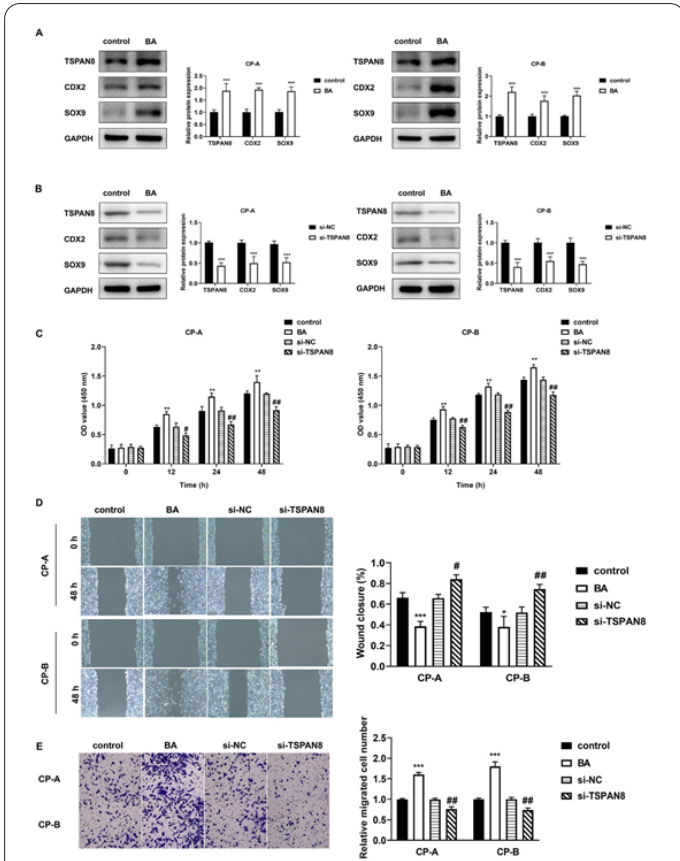


**Fig. 3.** Silencing of TSPAN8 inhibited BE cell proliferation, migration and invasion. (A) BA treatment promoted TSPAN8, CDX2 and SOX9 levels. (B) Silencing of TSPAN8 suppressed CDX2 and SOX9 levels. (C) Silencing of TSPAN8 inhibited BE cell proliferation. (D) Silencing of TSPAN8 inhibited cell migration. (E) Silencing of TSPAN8 inhibited cell invasion.

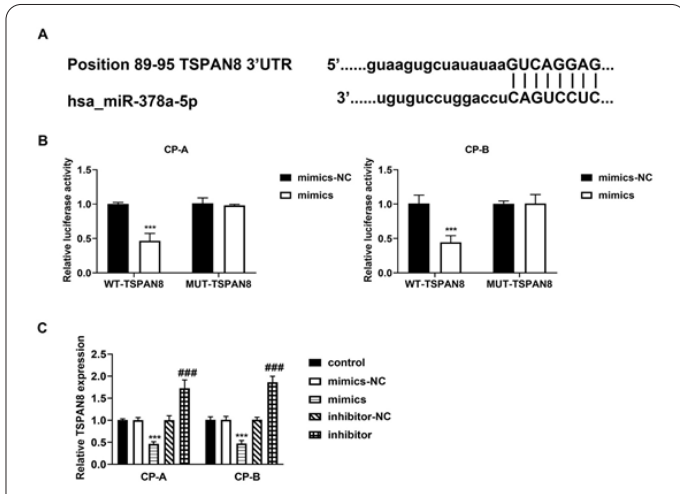


**Fig. 4.** TSPAN8 was a target for miR-378a-5p. (A) The potential binding sites of miR-378a-5p and TSPAN8. (B) The binding association of miR-378a-5p and TSPAN8 from dual-luciferase reporter assay. (C) miR-378a-5p inversely regulated TSPAN8 level in BE cells.

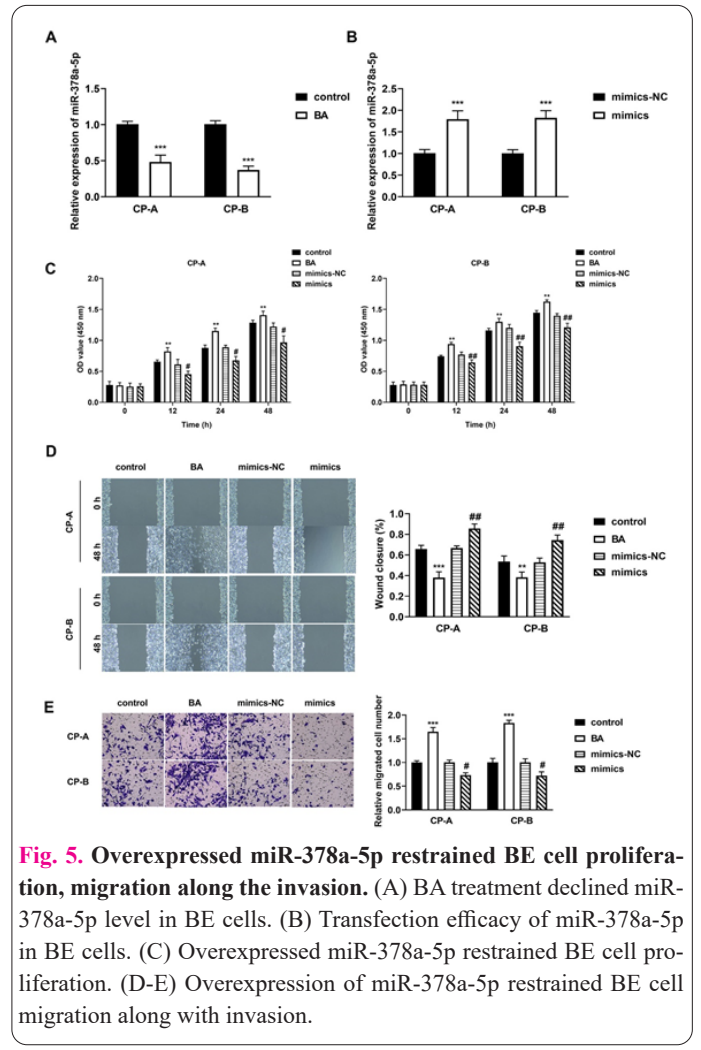


**Fig. 5.** Overexpressed miR-378a-5p restrained BE cell proliferation, migration along the invasion. (A) BA treatment declined miR-378a-5p level in BE cells. (B) Transfection efficacy of miR-378a-5p in BE cells. (C) Overexpressed miR-378a-5p restrained BE cell proliferation. (D-E) Overexpression of miR-378a-5p restrained BE cell migration along with invasion.

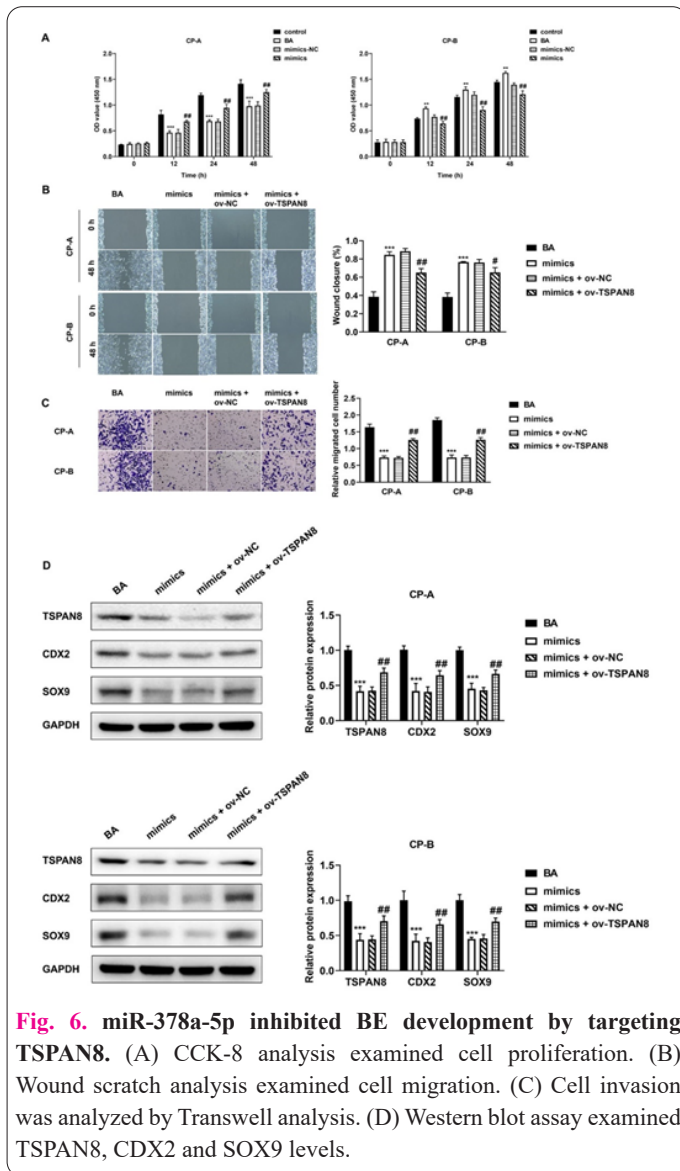
groups (Figure 4B). Additionally, the impact of miR-378a-5p on TSPAN8 level could be ascertained by RT-qPCR analysis. As displayed in Figure 4C, miR-378a-5p mimics could decrease TSPAN8 level whereas miR-378a-5p inhibitor enhanced TSPAN8 expression. Generally speaking, miR-378a-5p could target TSPAN8 as well as negatively regulate TSPAN8 levels in BE cells.

**3.5. miR-378a-5p increase hindered BE cell proliferation, migration along the invasion**

Moreover, the participation of miR-378a-5p in modulating BE cell progression was detected. First, after BA treatment, we discovered that miR-378a-5p level presented a reduction in CP-A and CP-B cells (Figure 5A). Moreover, the transfection efficacy of miR-378a-5p was verified through RT-qPCR analysis (Figure 5B). Next, the significance of miR-378a-5p on BE development could be proved by CCK-8, wound scratch as well as Transwell assays. As demonstrated in Figures 5C-5E, under BA conditions, BE cell proliferation, migration and invasion were markedly enhanced. Whereas, the enhancement induced by BA could be partially counterbalanced by miR-378a-5p overexpression. Together, we could deduce that miR-378a-5p alleviated BE progression by impeding cell proliferation, migration and invasion.

**3.6. miR-378a-5p targeted TSPAN8 to alleviate BE development**

The regulatory axis of miR-378a-5p/TSPAN8 in BE progression could be notarized by rescue experiments. Af-



ter co-transfection with miR-378a-5p mimics together with ov-TSPAN8 in CP-A and CP-B cells, a train of functional experiments was implemented subsequently. From the results in Figures 6A-6C, under BA conditions, miR-378a-5p mimics restrained BE cell proliferation, migration and invasion. However, the restraint triggered by miR-378a-5p mimics could be partially eliminated by ov-TSPAN8. Finally, BE-related proteins TSPAN8, CDX2 and SOX9 levels were examined via western blot assay. As illustrated in Figure 6D, relative to BA group, TSPAN8, CDX2 and SOX9 expressions were remarkably decreased in miR-378a-5p mimics; meanwhile, in comparison with mimics + ov-NC group, transfection with ov-TSPAN8 facilitated TSPAN8, CDX2 and SOX9 levels. Briefly, based on those experiments, it could be concluded that miR-378a-5p suppressed BE occurrence and development through targeting TSPAN8 level.

#### 4. Discussion

Though analyzing the GSE26886 dataset, we screened the most abundantly expressed gene TSPAN8 in BE samples. TSPAN8 is a class of membrane proteins consisting of 237 amino acid residues with a gene localized on 12q14.1-q21.1 [15]. It has been reported that TSPAN8 can bind to several molecules in the cytosol and intra-membrane to form tumor microenvironment and thus affect

tumor progression and metastasis [16]. For instance, TSPAN8 was found to be high-expressed in various solid tumors, containing colorectal cancer [17], breast cancer [18], melanoma [16], nasopharyngeal carcinoma [19], hepatocellular carcinoma [20] and has a significant role in promoting tumor metastasis. In esophageal carcinoma, TSPAN8 was up-regulated in tumor tissues as well [21]. In our study, we for the first time discovered up-regulated TSPAN8 in BE samples and in vitro cell models. The ROC analysis elucidated that TSPAN8 could distinguish BE subjects from healthy cases with high sensitivity, specificity and accuracy. Meanwhile, after knocking down TSPAN8 expression in CP-A and CP-B cells, we discovered that TSPAN8 could suppress cell proliferation and migration along invasion under BA environment.

Numerous literatures revealed that CDX2 is a critical factor in the pathogenesis of BE [22]. CDX2 protein played an important role in early differentiation as well as maintaining the intestinal epithelium by modulating the transcription of intestine-specific genes [23]. Usually, CDX2 was a sensitive indicator of upper gastrointestinal epithelial dysplasia and helped in the diagnosis of BE [24]. SOX9 was a transcription factor located in Paneth cells of the intestinal crypts and potentially in stem cells [25]. Previous studies found that SOX9 expression was detected in patients with BE [26]. It has also been reported that SOX9 is implicated in the pathogenesis of BE and can be a target gene of the Hedgehog (HH) signaling pathway [14]. In our research, after stimulating CP-A and CP-B cells with BA, SOX9 and CDX2 levels were prominently increased, implying the construction of BE in vitro model was successful. Also, the knockdown of TSPAN8 could hinder SOX9 and CDX2 expressions, verifying the hypothesis that TSPAN8 could aggravate BE development.

miRNAs belong to a group of non-coding RNAs with 18 to 25 nucleotides in length and can degrade or suppress target mRNAs' translation through base-pairing with their 3' UTR sites [27]. Numerous studies have shown that miRNAs have crucial roles in various physiological and pathological processes, including metabolism, proliferation, differentiation, and carcinogenesis [28]. These findings suggested that miRNAs can be used as candidate molecular markers for the diagnosis and prognosis of numerous diseases [29]. miR-378a-5p has been documented to be an anti-tumor factor in colorectal cancer [30], breast cancer [31], oral squamous cell carcinoma [32], hepatocellular carcinoma [33] along with renal cell carcinoma [34]. In esophageal squamous cell carcinoma, Wang et al. [35] illustrated that miR-378a-5p could deplete lipogenesis and tumorigenesis as well. In our experiments, through TargetScan online tool, we discovered that miR-378a-5p might target TSPAN8. Moreover, the dual-luciferase reporter assay as well as rescue assays validated the targeted relationship of miR-378a-5p and TSPAN8. The functional experiments elucidated that miR-378a-5p presented low expression in BE specimens and cells, serving as a feasible high-sensitive biomarker for BE detection. Meanwhile, overexpression of miR-378a-5p could inversely regulate TSPAN8 level to restrain BE development.

Collectively, our study was the first to report that miR-378a-5p could alleviate BE progression through targeting TSPAN8 and may be a hopeful therapeutic target for BE treatment.

## Informed Consent

The authors report no conflict of interest.

## Availability of data and material

We declared that we embedded all data in the manuscript.

## Authors' contributions

XX conducted the experiments and wrote the paper; WD conceived, designed the study and revised the manuscript.

## Funding

None.

## Acknowledgement

We thanked Xianyang Hospital of Yan'an University approval our study.

## References

- Clermont M, Falk GW (2018) Clinical guidelines update on the diagnosis and management of Barrett's esophagus. *Dig Dis Sci* 63(8):2122–2128. doi: 10.1007/s10620-018-5070-z
- Que J, Garman KS, Souza RF, Spechler SJ (2019) Pathogenesis and Cells of Origin of Barrett's Esophagus. *Gastroenterology* 157(2):349–364.e1. doi: 10.1053/j.gastro.2019.03.072
- Yamasaki T, Sakiani S, Maradey-Romero C, Mehta R, Sandhu D, Ganocy S, et al (2020) Barrett's esophagus patients are becoming younger: analysis of a large United States dataset. *Esophagus* 17(2):190–196. doi: 10.1007/s10388-019-00707-7
- Chen X, Zhu LR, Hou XH (2009) The characteristics of Barrett's esophagus: an analysis of 4120 cases in China. *Dis Esophagus* 22(4):348–353. doi: 10.1111/j.1442-2050.2008.00924.x
- Schlottmann F, Molena D, Patti MG (2018) Gastroesophageal reflux and Barrett's esophagus: a pathway to esophageal adenocarcinoma. *Updates Surg* 70(3):339–342. doi: 10.1007/s13304-018-0564-y
- Tróchez Mejía CF, Hernández Guerrero A, Herrera Servin M (2020) Development of Barrett's esophagus after a total gastrectomy. *Rev Esp Enferm Dig* 112(12):954. doi: 10.17235/reed.2020.7041/2020
- Krüger L, Pridgen TA, Taylor ER, Garman KS, Blikslager AT (2020) Lubiprostone protects esophageal mucosa from acid injury in porcine esophagus. *Am J Physiol Gastrointest Liver Physiol* 318(4):G613–G623. doi: 10.1152/ajpgi.00086.2019
- Iizuka T, Suzuki Y, Kikuchi D, Hoshihara Y, Ohkura Y, Ueno M (2020) Columnar epithelium morphology after esophagectomy: clinical insight into the development of Barrett's esophagus. *Esophagus* 17(4):392–398. doi: 10.1007/s10388-020-00742-9
- Funabashi M, Grove TL, Wang M, Varma Y, McFadden ME, Brown LC, et al (2020) A metabolic pathway for bile acid dehydroxylation by the gut microbiome. *Nature* 582(7813):566–570. doi: 10.1038/s41586-020-2396-4
- Jiao N, Baker SS, Chapa-Rodriguez A, Liu W, Nugent CA, Tsompana M, et al (2018) Suppressed hepatic bile acid signaling despite elevated production of primary and secondary bile acids in NAFLD. *Gut* 67(10):1881–1891. doi: 10.1136/gutjnl-2017-314307
- Quilty F, Freeley M, Gargan S, Gilmer J, Long A (2021) Deoxycholic acid induces proinflammatory cytokine production by model oesophageal cells via lipid rafts. *J Steroid Biochem Mol Biol* 214:105987. doi: 10.1016/j.jsbmb.2021.105987
- Peng S, Huo X, Rezaei D, Zhang Q, Zhang X, Yu C, et al (2014) In Barrett's esophagus patients and Barrett's cell lines, ursodeoxycholic acid increases antioxidant expression and prevents DNA damage by bile acids. *Am J Physiol Gastrointest Liver Physiol* 307(2):G129–G139. doi: 10.1152/ajpgi.00085.2014
- Tamagawa Y, Ishimura N, Uno G, Aimi M, Oshima N, Yuki T, et al (2016) Bile acids induce Delta-like 1 expression via Cdx2-dependent pathway in the development of Barrett's esophagus. *Lab Invest* 96(3):325–337. doi: 10.1038/labinvest.2015.137
- Huang J, Liu H, Sun T, Fang JY, Wang J, Xiong H (2019) Omeprazole prevents CDX2 and SOX9 expression by inhibiting hedgehog signaling in Barrett's esophagus cells. *Clin Sci (Lond)* 133(3):483–495. doi: 10.1042/CS20180828
- Heo K, Lee S (2020) TSPAN8 as a Novel Emerging Therapeutic Target in Cancer for Monoclonal Antibody Therapy. *Biomolecules* 10(3):388. doi: 10.3390/biom10030388
- El Kharbili M, Agaësse G, Barbolat-Boutrand L, Pommier RM, de la Fouchardière A, Larue L, et al (2019). Tspan8- $\beta$ -catenin positive feedback loop promotes melanoma invasion. *Oncogene* 38(20):3781–3793. doi: 10.1038/s41388-019-0691-z
- Zhang HS, Liu HY, Zhou Z, Sun HL, Liu MY (2020) TSPAN8 promotes colorectal cancer cell growth and migration in LSD1-dependent manner. *Life Sci* 241:117114. doi: 10.1016/j.lfs.2019.117114
- Voglstatter M, Thomsen AR, Nouvel J, Koch A, Jank P, Navarro EG, et al (2019) Tspan8 is expressed in breast cancer and regulates E-cadherin/catenin signalling and metastasis accompanied by increased circulating extracellular vesicles. *J Pathol* 248(4):421–437. doi: 10.1002/path.5281
- Lin X, Bi Z, Hu Q, Li Q, Liu J, Luo ML, et al (2019) TSPAN8 serves as a prognostic marker involving Akt/MAPK pathway in nasopharyngeal carcinoma. *Ann Transl Med* 7(18):470. doi: 10.21037/atm.2019.08.02
- Cai S, Deng Y, Peng H, Shen J (2021) Role of Tetraspanins in Hepatocellular Carcinoma. *Front Oncol* 11:723341. doi: 10.3389/fonc.2021.723341
- Botelho NK, Schneiders FI, Lord SJ, Freeman AK, Tyagi S, Nancarrow DJ, et al (2010) Gene expression alterations in formalin-fixed, paraffin-embedded Barrett esophagus and esophageal adenocarcinoma tissues. *Cancer Biol Ther* 10(2):172–179. doi: 10.4161/cbt.10.2.12166
- Gil-Gómez G, Fassan M, Nonell L, Garrido M, Climent M, Anglada R, et al (2021) miR-24-3p regulates CDX2 during intestinalization of cardiac-type epithelium in a human model of Barrett's esophagus. *Dis Esophagus* 34(7):doab005. doi: 10.1093/dote/doab005
- Li T, Guo H, Li H, Jiang Y, Zhuang K, Lei C, et al (2019) MicroRNA-92a-1-5p increases CDX2 by targeting FOXD1 in bile acids-induced gastric intestinal metaplasia. *Gut* 68(10):1751–1763. doi: 10.1136/gutjnl-2017-315318
- Valente P, Garrido M, Gullo I, Baldaia H, Marques M, Baldaque-Silva F, et al (2015) Epithelial dysplasia of the stomach with gastric immunophenotype shows features of biological aggressiveness. *Gastric Cancer* 18(4):720–728. doi: 10.1007/s10120-014-0416-5
- Han SJ, Kim M, D'Agati VD, Lee HT (2020) Norepinephrine released by intestinal Paneth cells exacerbates ischemic AKI. *Am J Physiol Renal Physiol* 318(1):F260–F272. doi: 10.1152/ajprenal.00471.2019
- Zhang X, Westerhoff M, Hart J (2015) Expression of SOX9 and CDX2 in nongoblet columnar-lined esophagus predicts the detection of Barrett's esophagus during follow-up. *Mod Pathol* 28(5):654–661. doi: 10.1038/modpathol.2014.157
- Khodakarimi S, Zarebkohan A, Kahroba H, Omrani M, Sepasi T, Mohaddes G, et al (2021) The role of miRNAs in the regulation of autophagy in autoimmune diseases. *Life Sci* 287:119726. doi: 10.1016/j.lfs.2021.119726

28. Machado IF, Teodoro JS, Palmeira CM, Rolo AP (2020) miR-378a: a new emerging microRNA in metabolism. *Cell Mol Life Sci* 77(10):1947–1958. doi: 10.1007/s00018-019-03375-z
29. Chen W, Song J, Bian H, Yang X, Xie X, Zhu Q, et al (2020) The functions and targets of miR-212 as a potential biomarker of cancer diagnosis and therapy. *J Cell Mol Med* 24(4):2392–2401. doi: 10.1111/jcmm.14966
30. Li K, Zhang J, Zhang M, Wu Y, Lu X, Zhu Y (2021) miR-378a-5p inhibits the proliferation of colorectal cancer cells by downregulating CDK1. *World J Surg Oncol* 19(1):54. doi: 10.1186/s12957-021-02166-w
31. Zheng S, Li M, Miao K, Xu H (2020) lncRNA GAS5-promoted apoptosis in triple-negative breast cancer by targeting miR-378a-5p/SUFU signaling. *J Cell Biochem* 121(3):2225–2235. doi: 10.1002/jcb.29445
32. Cui Z, Liu QL, Sun SQ, Jiao K, Liu DR, Zhou XC, Huang L (2020) MiR-378a-5p inhibits angiogenesis of oral squamous cell carcinoma by targeting KLK4. *Neoplasma* 67(1):85–92. doi: 10.4149/neo\_2019\_190306N191
33. Zou H, Yang L (2020) miR-378a-5p improved the prognosis and suppressed the progression of hepatocellular carcinoma by targeting the VEGF pathway. *Transl Cancer Res* 9(3):1558–1566. doi: 10.21037/tcr.2020.01.46
34. Pan X, Zhao L, Quan J, Liu K, Lai Y, Li Z, et al (2019) MiR-378a-5p acts as a tumor suppressor in renal cell carcinoma and is associated with the good prognosis of patients. *Am J Transl Res* 11(4):2207–2218.
35. Wang X, Liu H, Zhang Q, Zhang X, Qin Y, Zhu G, et al (2021) LINC00514 promotes lipogenesis and tumor progression in esophageal squamous cell carcinoma by sponging miR-378a-5p to enhance SPHK1 expression. *Int J Oncol* 59(5):86. doi: 10.3892/ijo.2021.5266